January 1, 2009

Self-assembly of fluorocarbon-coated FePt nanoparticles for controlling structure and wettability of surfaces

B Samanta
Y Ofir
D Patra
VM Rotello

Self-assembly of fluorocarbon-coated FePt nanoparticles for controlling structure and wettability of surfaces†‡

Bappaditya Samanta, Yuval Ofir, Debabrata Patra and Vincent M. Rotello*

Received 20th May 2008, Accepted 17th June 2008
First published as an Advance Article on the web 29th July 2008
DOI: 10.1039/b808494g

Controlled self-assembly of fluorinated FePt nanoparticles from different solvent mixtures has been used to create superhydrophobic surfaces with varying topology and stickiness towards water. The ability to tune surface stickiness provides a means for fluid handling, as demonstrated by surface-to-surface transfer of water droplets.

1. Introduction

Inorganic nanoparticles (NPs) are highly attractive as potential building blocks for future nanotechnology, due to their controllable properties, which change with core material, size, and shape.[1] Apart from the size and shape control, self-assembly of these NPs is increasingly recognized for the modulation of novel collective properties due to controlled interaction between the NPs.[2] Self-assembly has been used for organizing NPs into multidimensional close-packed ordered arrays by simply controlling the evaporation of the dispersing medium.[3]

Superhydrophobic surfaces, with water contact angles (CAs) higher than 150°, have attracted great interest in material research for their potential applications, ranging from self-cleaning surfaces to microfluidic devices.[4,5] These surfaces, usually exhibit both large water CA and small water sliding angle (SA), and are normally achieved by combining appropriate surface roughness and deposition of low surface energy materials, *e.g.* fluorinated compounds.[6,7]

Surfaces with large SA that exhibit sufficiently high adhesive force to water likewise attracted attention for applications in liquid transport and analysis of very small volumes of water samples. Recently, Jiang *et al.* have reported superhydrophobic surfaces formed by aligned polystyrene nanotubes with CAs of up to 162°, that even when tilted by 90° and upside down did not release the water droplet sitting on it.[8] In another report, Guo *et al.* showed a sticky superhydrophobic surface from a hydrophilic aluminium alloy.[9]

Recently, we have shown the formation of hydrophobic to superhydrophobic surfaces based on self-assembly of ~2.5 nm FePt NPs with varying amount of fluorinated ligands by controlling solvent-evaporation rate or deposition method.[10] Fully fluorinated FePt NPs showed crystalline assemblies ranging from sub-micrometre size to several microns, achieving superhydrophobic surfaces by a simple solvent evaporation.

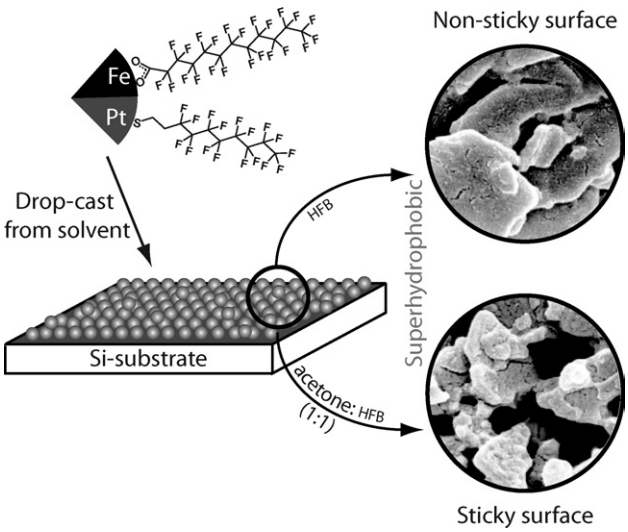

Scheme 1 Drop-casting of fluorocarbon-coated FePt NPs from different solvent systems: (A) hexafluorobenzene (HFB), (B) 1 : 1 mixture of acetone and HFB.

Herein we demonstrate control over topology and stickiness of superhydrophobic surfaces formed by self-assembly of fully fluorinated FePt NPs from different solvent mixtures (Scheme 1). By simply varying the solvent used for drop-casting, a wide range of surface morphologies were produced. This change in morphology is functionally significant; superhydrophobic surfaces can be formed featuring very low or very high adhesion to water using a single precursor.

2. Experimental

2.1. Materials

HFB was purchased from Oakwood Chemicals. All other starting materials were purchased from Sigma-Aldrich except iron pentacarbonyl, and dodecylamine, which were bought from Fischer Scientific and used without further purification.

2.2. NPs synthesis and films preparation

Synthesis of FePt NPs. The synthesis of oleic acid- and oleylamine-coated NPs and further place-exchange reaction with

Department of Chemistry, University of Massachusetts, Amherst, MA 01003, USA. E-mail: rotello@chem.umass.edu; Fax: +1 413-545-4490; Tel: +1 413-545-2058

† This paper is part of a *Soft Matter* theme issue on Self-Assembly. Guest editor: Bartosz Grzybowski.

‡ Electronic supplementary information (ESI) available: Small-angle X-ray scattering of NP films, and a movie of a water droplet transfer process. See DOI: 10.1039/b808494g

fluorinated ligands has been reported before.[10] In brief: under an argon atmosphere, platinum acetylacetonate (197 mg, 0.5 mmol), 1,2-hexadecanediol (390 mg, 1.5 mmol) and dioctylether (20 mL) were mixed and heated to 100 °C. Oleic acid (0.16 mL, 0.5 mmol), oleyl amine (0.17 ml, 0.5 mmol), and $Fe(CO)_5$ (0.13 mL, 1 mmol) were added at this temperature. The mixture was further refluxed for 30 min, cooled down to room temperature and precipitated using ethanol. NPs were purified by dispersing them in hexane followed by re-precipitation using ethanol. NPs were finally re-dispersed in dichloromethane (DCM).

Place-exchange reaction of FePt. In brief: 50 mg of the alkyl-coated FePt NPs were dissolved in 5 mL DCM with 200 mg of perfluorododecanoic acid in 0.5 mL of acetone and 200 mg of 1*H*,1*H*,2*H*,2*H*-perfluorodecanethiol. The resulting mixture was purged with argon and heated for 2 days at 40 °C in a closed vial. Solvents were removed under reduced pressure. Excess ligands were removed by washing the NPs with acetone. The resulting black residue was re-dispersed in HFB.

Surface coating. NP films were fabricated from different solvent systems by drop casting ~100 μL solutions on freshly cleaned silicon substrates. Solvents were allowed to evaporate in an ambient environment. After complete solvent evaporation, samples were placed in high vacuum to remove any trapped solvent inside the NPs film.

2.3. Characterization

Field emission scanning electron microscopy (FESEM) images were acquired on a JEOL 6320FXV FESEM at an accelerating voltage of 5 kV after gold sputtering. Water CAs were measured on a VCA-Optima XE Surface Analysis System (AST Products Inc.) at ambient temperature. For small-angle X-ray scattering (SAXS) measurements, samples were prepared by drop-casting the NP solutions onto a ~1 cm^2 piece of Mylar film. The sample was allowed to fully dry. Spectra were acquired on a molecular metrology instrument producing an X-ray λ of 0.0154 nm. The scattering intensity is presented as a function of the wave vector $q = (4\pi/\lambda)\sin(2\theta/2)$, where 2θ is the scattering angle. The q value of maximum intensity was converted to distance through the relationship $q = 2\pi/d$, where d is the distance in nm.

3. Results and discussion

Fluorocarbon-coated ~2.5 nm FePt NPs were synthesized by exchanging the originally coated oleic acid- and oleylamine-functionalized FePt NPs with perfluorodecanethiol and perfluorododecanoic acid following a reported protocol.[10] Verification of successful place-exchange reaction was confirmed by X-ray photoelectron spectroscopy measurements and thermal gravimetric analysis as reported before. NPs dispersion in HFB ($FePt_{HFB}$) or 1 : 1 mixtures of pentanol, butanol or acetone with HFB ($FePt_{0.5P}$, $FePt_{0.5B}$ and $FePt_{0.5A}$, respectively) were drop-casted onto a clean silicon substrate; followed by a simple solvent evaporation.

The surface wettability of the as-prepared substrates was studied by static (θ_s), advancing (θ_A) and receding (θ_R) CA measurements, as well as measuring the water SA, reported in Table 1. θ_s of all NP films showed no dependency on the composition of the dispersing medium and was documented as ~150°. Examination of the θ_A and θ_R CA measurements allowed us to evaluate the hysteretic nature ($\theta_A - \theta_R$) of the different films formed. The $FePt_{HFB}$, $FePt_{0.5P}$, $FePt_{0.5B}$ and $FePt_{0.5A}$, films showed contact angle hysteresis of 19°, 11°, 13° and 121°, respectively, which is in agreement with the measured SAs of 15°, 9°, 12° and no sliding, respectively.

Table 1 Static (θ_s), advancing (θ_A), receding (θ_R) CAs, and SA of various NP films fabricated by depositing NPs from different solvent systems

NPs film	θ_S ±3/°	θ_A ±3/°	θ_R ±3/°	$\theta_A - \theta_R$/°	SA/°
$FePt_{HFB}$	156	163	144	19	15
$FePt_{0.5\ P}$	148	148	137	11	9
$FePt_{0.5B}$	151	155	142	13	12
$FePt_{0.5A}$	152	156	35	121	—

FESEM was used to examine the effect of the different solvent systems on the films morphology. Fig. 1 shows FESEM analysis of the films, indicating different degrees of surface roughness and porosity of the samples. The $FePt_{HFB}$ film showed crystalline NP assemblies ranging from sub-micrometre to several microns (Fig. 1a). A relatively flat surface consisting of cracks, as well as star-shaped features of 60–80 microns was observed in the case of $FePt_{0.5P}$ films (Fig. 1b). On the other hand, the $FePt_{0.5B}$ film showed ribbon-like structures of a few microns in length with micron-sized crystalline aggregates (Fig. 1c). The highly rough crystalline NPs aggregates found in $FePt_{HFB}$, $FePt_{0.5P}$, $FePt_{0.5B}$ film surface allows the water to partially sit on the air pockets trapped between the crystals, rendering the superhydrophobicity with low SA.

In contrast, the $FePt_{0.5A}$ surface showed relatively small crystalline NP assemblies with more void spaces, nano-orifices, (Fig. 1d) compared to the $FePt_{HFB}$. Experimental results show

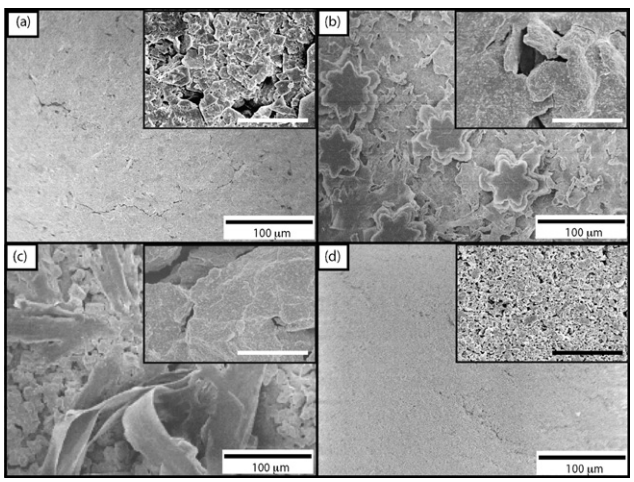

Fig. 1 FESEM images of silicon surface coated with (a) $FePt_{HFB}$ film, (b) $FePt_{0.5P}$ film (c) $FePt_{0.5B}$ film and (d) $FePt_{0.5A}$ film. Insets show high-resolution FESEM images (scale bar represents 10 μm).

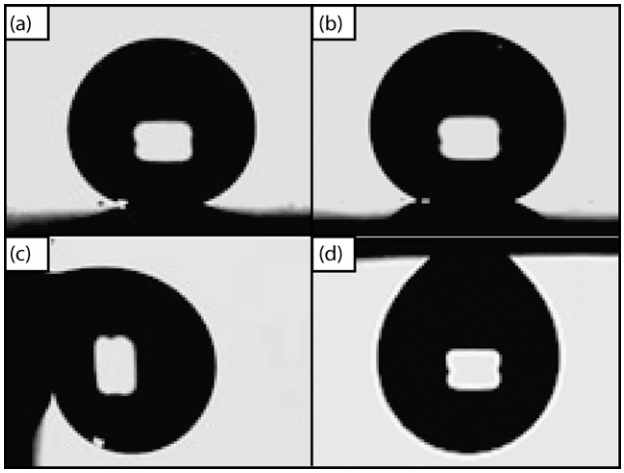

Fig. 2 (a) Profile of water droplet on $FePt_{HFB}$ surface with a water CA of 156°. Shapes of water droplet on $FePt_{0.5A}$ surface with different tilt angles: (b) 0°, (c) 90° and (d) 180°.

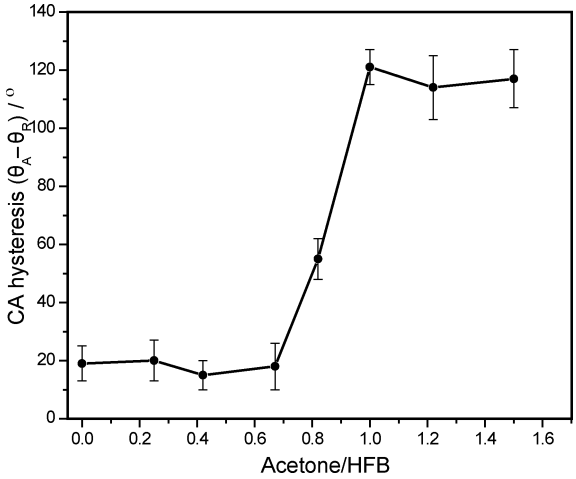

Fig. 3 Plot of water CA hysteresis (θ_A 1 θ_R) *versus* acetone–HFB ratio in the NPs solution.

that the water droplet does not slide off the surface even when the surface is tilted vertically (Fig. 2c) or turned upside down (Fig. 2d) when the critical weight of water droplet is as high as 6 mg, indicating a strong adhesion between the surface and the water droplet. Though a completely different morphology is observed with $FePt_{HFB}$ and $FePt_{0.5A}$ surfaces, SAXS confirms that both of them have the same inter-NP spacing of 4.7 nm (see ESI‡). These SAXS data suggests that the local environment of the NPs remains unaltered and only macroscopic structure of the surface changes during the assembly process. We believe that the enhancement of capillary forces between the nano-orifices of the $FePt_{0.5A}$ surface and the water leads to the high water adhesion.

The difference in topology and surface structures of the samples is attributed to the different boiling points of the solvents used in the mixtures. For the $FePt_{HFB}$, $FePt_{0.5P}$, $FePt_{0.5B}$ systems, the size and structures of the crystallites is dictated by the evaporation of the HFB component. Since the NPs are only marginally soluble in butanol and pentanol, and their boiling points are higher than that of HFB, the NPs are slowly assembled into micron-sized crystals as the HFB evaporates. In the case of the $FePt_{0.5A}$ system, the precipitation of the NPs occurs from a co-solvent, which gives rise to fast precipitation and small crystallites.

To assess the effect of acetone on the NPs assembly process, we have studied the properties of surfaces formed with a varied ratio of acetone to HFB. Films made from HFB–acetone ratios of 1 : 0.25, 1 : 0.42, 1 : 0.67, and 1 : 0.82 show superhydrophobic character (θ_s more than 150°) with contact angle hysteresis of 20°, 15°, 18° and 55°, respectively, again in agreement with measured SAs of 18°, 17°, 20° and 50°, respectively. NP films deposited from 1 : 1 ratio of acetone–HFB and above (over 50% acetone), do not release the droplet, which supports the contact angle hysteresis of more than 110° (Fig. 3). This experiment suggests that at least 50% acetone is needed to make the surface change its wetting characteristics, rendering it sticky to water. For low percentages of acetone in the mixture, quick evaporation of the acetone does not create a major change in the precipitation

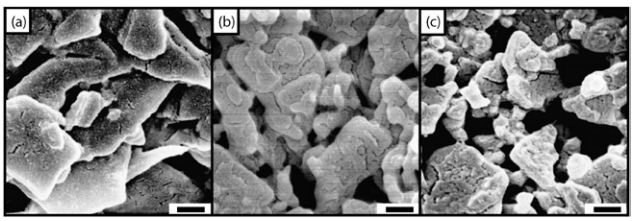

Fig. 4 High-resolution FESEM images of surfaces of NPs film deposited from (a) HFB, and mixtures of HFB–acetone 1 : 0.82 (b) and 1:1 (c). Scale bars represent 200 nm.

conditions resulting in surface morphology similar to that formed by $FePt_{HFB}$ only and similar wetting behaviour. As before for 50% and higher acetone in the mixture, the evaporation of the low boiling point acetone creates an unstable solution that precipitates to form a different morphology and wetting character. Fig. 4 shows high-resolution FESEM images of the surfaces drop-casted from (a) HFB, (b) HFB–acetone ratio of 1 : 0.82, and (c) HFB–acetone ratio of 1 : 1. Moving from HFB to mixtures of HFB and acetone shows smaller size and more rounded crystallites coupled with a pronounced increase in the number of air voids between that contribute to the sticky nature of the surfaces.

To demonstrate the usefulness of the stickiness of the surface to water, we designed a liquid-transfer experiment (Fig. 5). Two superhydrophobic surfaces, one non-sticky and another sticky, were fabricated using $FePt_{HFB}$ and $FePt_{0.5A}$, respectively. A droplet of water is placed on the $FePt_{HFB}$ surface (Fig. 5a) and then brought close to a sticky $FePt_{0.5A}$ surface. Upon contact the water droplet sticks to the $FePt_{0.5A}$ surface (Fig. 5b and c), and finally transferred to it when the substrates are pulled apart (Fig. 5d, a movie of the process is available in the ESI‡).

4. Conclusions

In summary, we have presented a very simple method for forming superhydrophobic sticky and non-sticky surfaces based

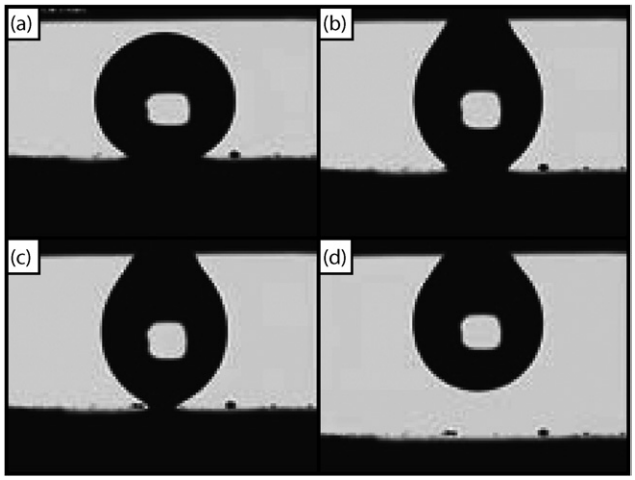

Fig. 5 Stepwise transfer of a water droplet from non-sticky superhydrophobic $FePt_{HFB}$ surface (bottom substrate) to a sticky superhydrophobic $FePt_{0.5A}$ surface (top substrate) from (a) to (d).

on self-assembly of fluorocarbon-coated FePt NPs from different solvent systems. Using different solvent mixture compositions allowed us to control the surface morphology of the drop-casted films formed, which in turn controls the wetting of the surfaces. The use of the NPs building blocks allows control of both micron and nanometre length scale morphology, while also reducing the surface energy using fluorinated ligands. These results offer an opportunity to further understand the wettability of solid surfaces based on NPs assembly. This methodology can be easily transferred to other NP systems that offer also optical, electrical and magnetic properties.

Acknowledgements

This research was funded by CHE-0518487, MRSEC facilities, and the NSF Center for Hierarchical Manufacturing at the University of Massachusetts DMI-0531171

References

1 (*a*) A. R. Tao, S. Habas and P. Yang, *Small*, 2008, **4**, 310–325; (*b*) Y.-W. Jun, J.-W. Seo and J. Cheon, *Acc. Chem. Res.*, 2008, **41**, 179–189.
2 (*a*) E. V. Shevchenko, D. V. Talapin, A. L. Rogach, A. Kornowski, M. Haase and H. Weller, *J. Am. Chem. Soc.*, 2002, **124**, 11480–11485; (*b*) J. J. Urban, D. V. Talapin, E. V. Shevchenko, C. R. Kagan and C. B. Murray, *Nat. Mater.*, 2007, **6**, 115–121; (*c*) J. M. Luther, M. Law, Q. Song, C. L. Perkins, M. C. Beard and A. J. Nozik, *ACS Nano*, 2008, **2**, 271–280.
3 (*a*) E. V. Shevchenko, J. B. Kortright, D. V. Talapin, S. Aloni and A. P. Alivisatos, *Adv. Mater.*, 2007, **19**, 4183–4188; (*b*) Z. Y. Tang and N. A. Kotov, *Adv. Mater.*, 2005, **17**, 951–962; (*c*) K. Soulantica, A. Maisonnat, M. C. Fromen, M. J. Casanove and B. Chaudret, *Angew. Chem., Int. Ed.*, 2003, **42**, 1945–1949; (*d*) D. V. Talapin, E. V. Shevchenko, C. B. Murray, A. Kornowski, S. Forster and H. Weller, *J. Am. Chem. Soc.*, 2004, **126**, 12984–12988.
4 (*a*) Z. G. Guo, F. Zhou, J. C. Hao and W. M. Liu, *J. Am. Chem. Soc.*, 2005, **127**, 15670–15671; (*b*) N. J. Shirtcliffe, G. McHale, M. I. Newton, G. Chabrol and C. C. Perry, *Adv. Mater.*, 2004, **16**, 1929–1932; (*c*) T. L. Sun, L. Feng, X. F. Gao and L. Jiang, *Acc. Chem. Res.*, 2005, **38**, 644–652.
5 (*a*) K. Hashimoto, *J. Phys. Chem. B*, 2001, **105**, 1984–1990; (*b*) M. Miwa, A. Nakajima, A. Fujishima, K. Hashimoto and T. Watanabe, *Langmuir*, 2000, **16**, 5754–5760; (*c*) A. Nakajima, A. Fujishima, K. Hashimoto and T. Watanabe, *Adv. Mater.*, 1999, **11**, 1365–1368; (*d*) P. Roach, N. J. Shirtcliffe and M. I. Newton, *Soft Matter*, 2008, **4**, 224–240; (*e*) H. Liu, J. Zhaia and L. Jiang, *Soft Matter*, 2006, **2**, 811–821; (*f*) Y. Liu, J. Tang, R. Wang, H. Lu, L. Li, Y. Kong, K. Qi and J. H. Xin, *J. Mater. Chem.*, 2007, **17**, 1071–1078.
6 (*a*) D. O. H. Teare, C. G. Spanos, P. Ridley, E. J. Kinmond, V. Roucoules and J. P. S. Badyal, *Chem. Mater.*, 2002, **14**, 4566–4571; (*b*) K. Tsujii, T. Yamamoto, T. Onda and S. Shibuchi, *Angew. Chem., Int. Ed. Engl.*, 1997, **36**, 1011–1012; (*c*) L. Jiang, Y. Zhao and J. Zhai, *Angew. Chem., Int. Ed.*, 2004, **43**, 4338–4341; (*d*) I. Woodward, W. C. E. Schofield, V. Roucoules and J. P. S. Badyal, *Langmuir*, 2003, **19**, 3432–3438; (*e*) M. Li, Z. Wei and Lei Jiang, *J. Mater. Chem.*, 2008, **18**, 2276–2280.
7 (*a*) L. Feng, S. Li, H. Li, J. Zhai, Y. Song, L. Jiang and D. Zhu, *Angew. Chem., Int. Ed.*, 2002, **41**, 1221–1223; (*b*) R. M. Jisr, H. H. Rmaile and J. B. Schlenoff, *Angew. Chem., Int. Ed.*, 2005, **44**, 782–785; (*c*) L. Zhai, F. Ç. Cebeci, R. E. Cohen and M. F. Rubner, *Nano Lett.*, 2004, **4**, 1349–1353; (*d*) H. Chen, F. Zhang, S. Fu and X. Duan, *Adv. Mater.*, 2006, **18**, 3089–3093; (*e*) M. Li, J. Xu and Q. Lu, *J. Mater. Chem.*, 2007, **17**, 4772–4776.
8 M. Jin, X. Feng, L. Feng, T. Sun, J. Zhai, T. Li and L. Jiang, *Adv. Mater.*, 2005, **17**, 1977–1981.
9 Z.-G. Guo and W.-M. Liu, *Appl. Phys. Lett.*, 2007, **90**, 223111.
10 Y. Ofir, B. Samanta, P. Arumugam and V. M. Rotello, *Adv. Mater.*, 2007, **19**, 4075–4079.

